

ELECTROLYTE FLOW PATTERNS IN MOLTEN SALT ELECTROLYSIS CELLS

J. K. Koziol and D. R. Sadoway

Department of Materials Science and Engineering
Massachusetts Institute of Technology
Cambridge, Massachusetts 02139

From: "Energy Reduction Techniques in Metal Electrochemical Processes", Eds. R.G. Bautista and R.J. Wesely. The Metallurgical Society. Proceedings of a symposium sponsored by the Electrolytic Process Committee of The Metallurgical Society, held at the TMS-AIME Annual Meeting in New York February 24-28, 1985.

Solid electrodeposits from molten salts are typically incoherent, powdery, and/or dendritic. Fluid flow patterns in the electrolyte are being observed by a laser schlieren imaging technique in order to determine how mass transport affects the morphology of the metal deposit. Zinc is being deposited from a melt of $ZnCl_2$ -LiCl-KCl. Current density, electrolyte composition, anode-cathode separation, and electrode orientation are varied. The electrolyte flow patterns and the resulting zinc deposits are studied in relation to changes in process variables.

Introduction

The present study seeks to explain the poor quality of solid electro-deposits in molten salts through a consideration of the effects of fluid flow of the electrolyte. The same metal is being electrodeposited in separate experiments from aqueous solutions and molten salt electrolytes. The results of the aqueous work have been reported (1). Electrolyte flows are being observed by laser schlieren imaging. To permit this, special electrolysis cells and furnaces had to be designed and built. The result is an apparatus capable of following electrolyte flow patterns in molten salt electrolysis cells operating at temperatures up to 1000°C. Furthermore, the power requirements for this equipment, including the furnace, do not exceed 2 kW. As such, the system could be adapted for use aboard space laboratories.

Although the project nominally is studying electrodeposition, in many respects the broader question of the effect of convection on the stability of the solid-liquid interface is being addressed to some extent. Many theories of morphological stability have been proposed. However, it is very difficult to test these experimentally due to the severe physical limitations in precisely controlling the driving forces and due to the fact that such solid-liquid transformations cannot be observed directly in many media. For example, metals and semiconductors are not transparent to visible light.

The present study of zinc electrodeposition from molten salts is unique in several ways. First, in electrodeposition it is possible to control very precisely the driving force for transformation. Secondly, the thermal properties of molten salts match more closely those of metals or semiconductors than do organic or water based systems. Thirdly, this study relies on *in situ* observation with special emphasis on visualization of liquid phase motion. Fourthly, the effects of two different electrolytes (water and molten salt) on the process are compared.

Zinc has been chosen as the metal to study. It can be deposited both from aqueous chloride and molten chloride electrolytes; furthermore, both types of electrolyte system are transparent to visible light. This permits the use of noninvasive optical techniques of flow measurement.

Phase One of the zinc plating study was devoted to the electrorefining of zinc in acid zinc chloride solutions (1). During electrodeposition, the flow patterns in the electrolyte were observed by laser schlieren imaging for a variety of electrode configurations, electrolyte compositions, and applied overpotentials. This paved the way for Phase Two, which is the study of fluid flow patterns in the electrolyte during the electrodeposition of zinc from molten salt electrolysis.

Literature on Electrolyte Flow During Electrodeposition

Natural convection in electrochemical cells has received considerable attention. However, all of the experimental work has been done in aqueous systems.

The first theoretical treatment of the subject was put forward by J. N. Agar (2) and C. Wagner (3) in the late forties. Agar applied a dimensional analysis to the diffusion and convection processes governing mass transport to the electrode. His calculations yielded values of diffusion boundary layer thicknesses which were in agreement with experimentally-measured values. Wagner, on the other hand, was interested in the prediction

of limiting currents as a function of electrolyte concentration. The results of his rigorous theoretical treatment were in good agreement with data he had obtained experimentally by electrodepositing copper on vertical electrodes from H_2SO_4 - $CuSO_4$ aqueous solutions.

The same electrolyte and electrode arrangement were employed by Wilke, Tobias and Einsenberg (4,5), who showed that their experimental results, as well as Wagner's, can be represented with the help of the appropriate dimensionless parameters to yield:

$$Sh = A(Ra)^{1/4}, Ra < 10^{14} \quad (1)$$

where Sh is the Sherwood number, Ra is the Rayleigh number, and A = constant.

Denpo, Teruta, Fukunaka and Kondo (6) have recently shown that this correlation is valid for laminar flows. In their experiments they employed 1 m long electrodes (as compared to 0.4 m and 0.15 m long electrodes used by Wagner and Wilke, respectively) and demonstrated that turbulent flow takes place for $Ra > 2.5 \times 10^{15}$. Under such conditions the mass transfer rate data were best expressed by the correlation:

$$Sh = 0.0055(Ra)^{2/7}, Ra \geq 2.5 \times 10^{15} \quad (2)$$

Free convection mass transfer at horizontal electrodes was extensively studied by Wragg and coworkers (7-9). Using the laser schlieren technique of flow visualization, they observed the laminar-turbulent transition at $Ra = 3 \times 10^7$. Their results can be summarized by the following correlations:

$$Sh = 0.72(Ra)^{1/4} \text{ for the laminar region, } 3 \times 10^4 < Ra < 3 \times 10^7, \text{ and} \\ Sh = 0.18(Ra)^{1/3} \text{ for the turbulent region, } 3 \times 10^7 < Ra < 10^{12}.$$

Patrick, Wragg and Pargeter (10) investigated convection at inclined electrodes and found that for attached boundary layer flow conditions $Sh = 0.68(Ra \cos \theta)^{1/4}$ holds, where θ is the angle measured from the vertical. Regions of attached boundary extend from the horizontal, down-facing position (in the case of cathodic deposition, when the electrolyte becomes less dense) beyond the vertical position to slightly positive inclinations. Another interesting finding is the substantial increase in mass transfer rate for horizontal, upward-facing electrodes as compared to downward-facing ones.

Free convective mass transfer to a rod-shaped vertical electrode was investigated by Selman and Tavakoli-Attar (11). The measured mass transfer rates to the down-facing, disk-shaped portion of the electrode were found to dominate the overall mass transfer rate to such an extent that the same correlation is given for both: $Sh = 2.075 Gr^{0.167} Sc^{0.2}$, where Gr is the Grashof number and Sc is the Schmidt number. The Rayleigh number, Ra, is the product, $Sc \times Gr$. Selman's result is interesting in view of Patrick's findings. The Sherwood number is smallest for the downward-facing electrode; consequently, the vertical area should dominate the overall mass transfer rate. Selman found the opposite to be true, and as a possible explanation he proposed the effect of shrouding of the vertical wall by the upward flow of depleted electrolyte produced at the disk.

The hydrodynamic boundary layer for convective flow during electrolysis was investigated by Ibl and Muller (12). Suspending solid particles in the electrolyte and observing their movements, they were able to measure velocity

profiles and present the following correlation:

$$\frac{v_m X}{D} = A(Ra)^{2/5},$$

where v_m is the maximum velocity, D is the diffusion coefficient, and X is the distance from the lower edge of the vertical cathode.

The review of the literature pertaining to natural convection during electrolysis shows that mass transfer to the electrode is strongly affected by electrode orientation. Moreover, mass transfer rates for the multiple surface electrode are not additive.

Literature on Deposit Morphology

The first to investigate the phenomenon of dendritic growth in electrolyte systems was Wranglen (13), who by means of microscopic and X-ray studies described crystallographically the dendrites of various metals grown in aqueous solutions. He also introduced the idea of critical current density to describe the minimum current necessary for dendritic growth. According to Wranglen, dendrites can be expected to appear if the total current density is above this critical value, or if the current is not uniformly distributed over the entire electrode area and the local current densities exceed the critical value.

The effect of local current density variations on deposition at the limiting currents was shown by Kim and Journé (14), who observed dendrites growing from the edge of a rotating disk electrode, the location where current density was the highest. Wagner (15) showed theoretically that at total current densities lower than 1/3 of the limiting current density, the local current density for a vertical electrode in an aqueous solution is constant; consequently, dendritic growth is not possible under such conditions. This was experimentally determined by Ibl and coworkers (16). On the other hand, if total current density is higher than 1/3 of the limiting value, local variations in the current can result in localized dendritic growth.

Damianovic, Setty and Bockis (17) studied the mechanism and kinetics of copper electrocrystallization on different planes of a single crystal cathode. They found that for a given current density the electrode potential varies, depending upon the plane on which growth is occurring, until some thickness of electrodeposited is obtained. Beyond this thickness the potential stabilizes. It follows that the growth velocity of a particular crystal is dependent on its orientation. Consequently, the dendrites are expected to have a definite crystallographic direction, as was observed by Wranglen (13).

The first theory on dendritic growth in electrolytic systems was put forward by Barton and Bockris (18). It is based on the balance between spherical diffusion toward the dendrite tip and tip dissolution due to excess free surface energy for a very small radius. However, discrepancies were found between predicted and measured tip radii of silver dendrites grown in molten nitrate solutions. Hamilton (19) relaxed the cornerstone assumption of a spherical tip radius in the Barton-Bockris theory and replaced it with a paraboloid of revolution. Even with this improvement, he could not obtain an agreement with the experimental data. Later, Diggle, Despić and Bockris (20,21) extended the initial Barton-Bockris theory to a model that assumes that the initial diffusion-controlled growth of the dendrite precursors (growth pyramids increasing by layer or screw mechanisms) is replaced by activation-controlled rapid (but at

constant speed) growth after a certain size and tip radius are reached. The growth times predicted by this model were consistent with experimental values but still did not match them satisfactorily. Mansfield and Gilman (22), on the basis of *in situ* macroscopic observations, disputed the validity of the Diggle-Despić-Bockris (DDB) assumption that growth pyramids become dendritic precursors. They observed, on the contrary, a gradual slowing down of the pyramid growth rate, with dendrites initiating at whisker-like structures appearing between the pyramids.

It is evident that the above theories are imprecise, and that often their predictions are unrealistic. It is useful to recall the experimental observations pertaining to the dendrites growing in electrolytic systems. Landau (23) compiled them in the following manner:

- (1) Most metals plated to sufficient thickness will develop dendrites.
- (2) There is a correlation between exchange current densities (i_0) and the tendency to form dendrites. Metals of high i_0 form dendrites more readily.
- (3) There is a critical overpotential (or critical current density) which must be reached before dendrites appear, and this again can be correlated to i_0 .
- (4) Evolving dendrites exhibit an induction time before they become visible (initiation stage).
- (5) Once they are past the initiation stage, their growth is at a constant rate (propagation stage).
- (6) Tip shape is constant during the propagation stage.

Several attempts were made to understand dendritic behavior further, especially during the initiation stage. The work of Despić and Purenović (24) is essentially an extension of the DDB model. They concluded that the concept of a critical overpotential has a thermodynamic basis only for high i_0 metals and that the only limitations in the appearance of dendrites on the low i_0 metals are of a kinetic nature. Consequently, metals of high i_0 grow dendrites under activation control.

Aogaki, Kitazawa, Kose and Fueki (25) investigated cathodic deposition of metals under limiting current conditions. By applying the linear stability theory they concluded that cathodic electrocrystallization is always unstable. On the other hand, Huggins and Elwell (26) investigated the stability of a plane surface during electrocrystallization from molten salts. Their approach was based on the variation of chemical potential ahead of the interface during electrolysis. Their conclusion predicts stable growth in the case of high solute concentration and large electrochemical gradients at the crystal-solution interface.

From the above review it may be concluded that as current density is increased deposit morphology becomes coarser and more dendritic. This rule of thumb is in fact followed in practice (27), however it is an oversimplified view. For instance, large variations in local current density values can lead to the deposits expected for much higher overall current densities. Such local variations can occur either because of a variation in crystallographic orientation or because of nonuniform ionic fluxes to the electrode surface due to the electrolyte flow conditions. It is also apparent that the main direction of research on dendritic growth has been toward prediction of dendritic shape and the time characteristics of their evolution. Consequently the dependence of deposit morphology on convective flow has been left largely unexamined.

Zwilling (28) used forced convection in his attempts to change the deposit morphology of gadolinium in molten salt electrolysis by rotation of the cathode (up to 50 rev/min). However, working with an aqueous alkaline solution containing zincate ions, Naybour (29,30) was able to make significant al-

terations in zinc deposit characteristics by changing flow velocities in a forced flow system. For a given current density, increasing the flow rate changed the initially dendritic deposit to a nodular one; upon further flow rate increase the deposit became smooth.

No reports were found pertaining to deposit morphology dependence on free, buoyancy-driven convection in electrolytic systems; however, there has been some work in the related field of crystal growth (31).

Electrolyte Preparation

Observation of fluid flow patterns by laser schlieren imaging requires not simply that the electrolyte be transparent to visible light, but that the melt possess the highest degree of clarity and be free of solid particulates. In the molten salt system of interest, $ZnCl_2-LiCl-KCl$, the first two components are especially hygroscopic. Removal of water is not effected by simply heating the salts to a temperature greater than $100^\circ C$: the water is chemically bound. The presence of water in the salt can result in the formation of various species, for example, oxychlorides which chemically attack the glass container and which can be electrochemically oxidized, thereby disturbing the electrorefining operation of the cell. Upon heating, the oxychlorides also decompose to produce oxides which then obscure the melt.

The following salt dehydration procedure has been determined to be effective. The salts are first dried in a vacuum oven at $150^\circ C$ for 24 hours. Zinc chloride is then purified in a stream of HCl and Cl_2 gases at $250^\circ C$ followed by distillation under argon atmosphere. The final purification is conducted in the electrorefining vessel just before electrolysis begins. The temperature of the mixture is slowly raised to above its melting point ($340^\circ C$) while pure chlorine is bubbled through the melt. This is followed by an argon purge. Melt purity was analyzed by voltammetry on a solid platinum microelectrode.

Laser Schlieren Experiments

Schlieren methods (32,33) are standard visualization techniques used in the study of fluid flow. Variations in the index of refraction are detected and are interpreted as variations in fluid density or composition. The use of schlieren methods by electrochemists has been very limited. The present study employed the Toepler schlieren arrangement described in Reference 1. Electrolyte flow patterns were recorded during the electrodeposition of solid zinc from the molten salt electrolyte, $ZnCl_2-LiCl-KCl$. Experimental variables are current density, electrolyte composition, and cell geometry. Based on the results of the aqueous electrodeposition studies as well as reports in the literature, these parameters are identified as having the primary influence on cell performance in deposit quality. Current density varied over the range of 1 mA/cm^2 to 1 A/cm^2 ; the composition of the electrolyte varied from 5 mole % $ZnCl_2$ to 40 mole % $ZnCl_2$; anode-cathode separation varied from $1/4"$ to $1"$; and the electrode orientation varied from vertical to horizontal, in all cases "parallel-plate." Experiments are conducted to measure the fluid flow patterns and the electrolysis cell parameters, and to correlate this information with the morphology of the solid electrodeposit produced.

Results

Figure 1 shows photographs taken during an experiment conducted with horizontal electrodes spaced 14 mm apart. The upper electrode is the anode which is dissolving, while the lower electrode is the cathode onto which zinc

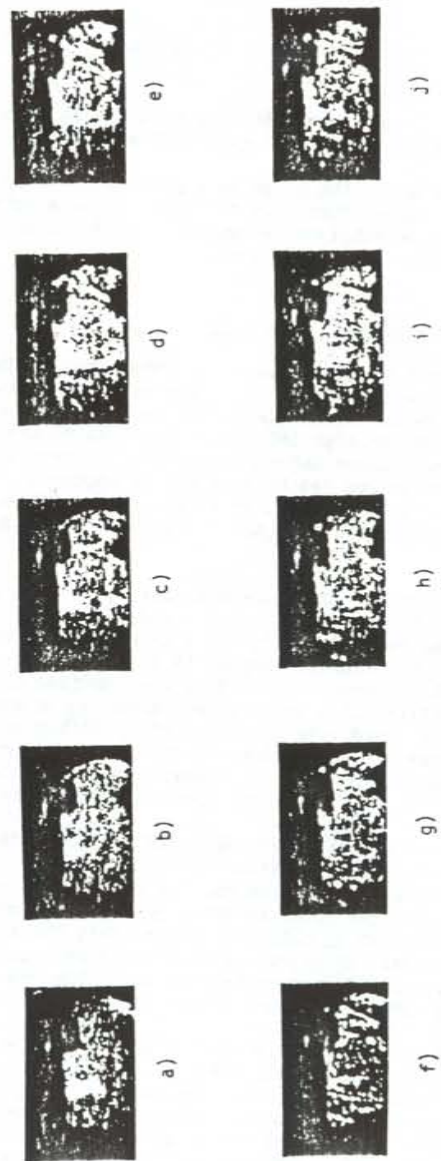


Figure 1. Schlieren images of electrolyte circulation during the galvanostatic electrodeposition of zinc from molten $ZnCl_2-KCl-LiCl$, $I=75 \text{ mA/cm}^2$. Anode surface is at the top of the photo frame; cathode surface is at the bottom. Time between frames, 20 s starting with $t=0$. Scale 1:1.

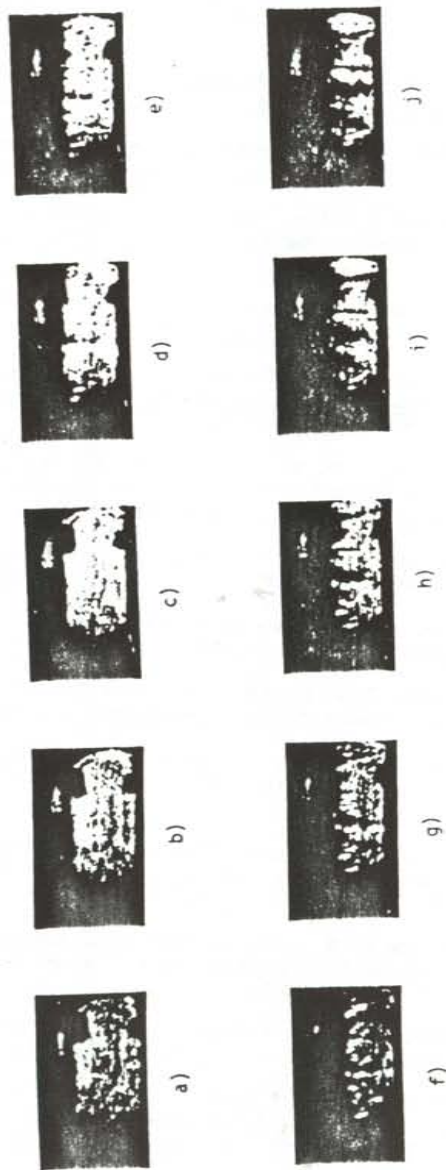


Figure 2. Schlieren images of electrolyte circulation during the galvanostatic electrodeposition of zinc from molten $ZnCl_2$ - KCl - $LiCl$, $i=125 \text{ mA/cm}^2$. Cathode surface is at the top of the photo frame; anode surface is at the bottom. Time between frames, 20 s starting with $t=0$. Scale 1:1.

is electrodeposited. The experiment was conducted galvanostatically at a current density of 75 mA/cm^2 . Photographs were taken at intervals of 20 seconds.

Figure 2 shows photographs taken during an experiment conducted again with horizontal electrodes spaced 14 mm apart. However, in this case the lower electrode is the anode, and the upper electrode is the cathode. Current density was 125 mA/cm^2 . Photographs were taken at intervals of 20 seconds.

These two cell geometries are presented because they represent extremes in fluid flow regimes. In the first case, with the cathode on the bottom, as the electrolyte next to the cathode is depleted of zinc, the density of this fluid decreases. With denser fluid above it, the "cathodic" melt eventually becomes hydrodynamically unstable and buoyancy-driven convection begins. In the second case, with the cathode on the top, as the electrolyte next to the cathode is depleted of zinc the density of this fluid decreases. Thus, a layer of less dense melt forms above the bulk electrolyte. This "cathodic" melt is stable and the electrodeposition proceeds under "diffusion control." The composition of the electrolyte in both experiments whose results are shown was held constant at 20 m/o $ZnCl_2$ -40 m/o KCl -40 m/o $LiCl$.

Discussion

In figures 1(a) and 2(a), photos taken as the electrodes were polarized, the schlieren image is not of uniform intensity but rather is composed of many dark and light spots that appear to fluctuate with time. It is as if the melt consisted of immiscible regions of varying index of refraction. This may be another unexplained optical behavior of molten salts akin to the broadband anomalous Rayleigh wing observed in Raman spectra of these melts.

Comparison of Figures 1 and 2 reveals that in the second experiment the concentration gradients are less severe, as it takes much longer for the schlieren intensities to develop.

In the experiment shown in Figure 1 a counterclockwise electrolyte circulation pattern was observed, evidently the consequence of buoyancy-driven convection. The time scale of the experiment was on the order of the induction time for dendrite growth, but effective electrolyte circulation repressed dendrite formation. The resulting deposit was rough but not dendritic.

In the experiment shown in Figure 2, large dendrites grew. This is consistent with the cell geometry which creates a diffusion-controlled electrolyte flow. It appears in some photographs that the dendrites emanating from the cathode have actually shorted to the anode; however, this could not have been the case, as no sharp decrease in cell voltage was measured. Frames f, g, and h of Figure 2 show that there are very severe gradients in index of refraction adjacent to the growing dendrites. This is a consequence of the steep concentration gradients in zinc ion alongside the advancing dendrites. This is not the condition at the dendrite tip, where there is an ample supply of zinc ions. Thus, schlieren imaging reveals that dendrite growth occurs normal to the concentration gradient. This is in conformity with prevailing theories.

Conclusions

Electrolyte flow patterns have been revealed by a laser schlieren imaging technique using specially developed hardware that could easily be adapted for use aboard space laboratories.

Schlieren patterns observed in molten salts are intrinsically different from those observed in aqueous solutions. In molten salts the dark field image is not featureless, but rather contains what appear to be time fluctuating gradients in the index of refraction.

In the vicinity of the growing dendrites, steep concentration gradients are detected normal to the principal growth direction as evidence of zinc depletion. In contrast, at the tip there is ample zinc for deposition. This is in conformity with general theories.

As the current density increases, the induction time for the onset of dendrite growth decreases. Changes in cell geometry have an identifiable effect on electrolyte circulation. For example, with horizontal parallel plate electrodes, inversion of anode and cathode changes the mode of mass transfer of zinc ions from diffusion control to buoyancy driven convection. The schlieren patterns confirm this. In low gravity crystal growth, this may be important in distinguishing Marangoni-driven flows from diffusional processes.

Acknowledgements

This work was supported by the National Aeronautics and Space Administration under grant number NSG-7645. Helpful discussions on the schlieren technique with Dr. Robert B. Owen, Space Sciences Laboratory, NASA Marshall Space Flight Center, are gratefully acknowledged.

References

1. A. A. Abdelmassih and D. R. Sadoway, "Laser Schlieren Studies of Aqueous Zinc Chloride Electrolysis," in *Chloride Electrometallurgy*, P. D. Parker, editor, TMS-AIME, Warrendale, PA, 1983, pp. 43-57.
2. J. N. Agar, "Diffusion and Convection at Electrodes," *Disc. Faraday Soc.*, 1 (1947), pp. 26-37.
3. C. Wagner, "The Role of Natural Convection in Electrolytic Processes," *Trans. Electrochem. Soc.*, 95 (1949), pp. 161-173.
4. C. R. Wilke, M. Eisenberg, and C. W. Tobias, "Correlation of Limiting Currents under Free Convection Conditions," *J. Electrochem. Soc.*, 100 (1953), pp. 513-523.
5. C. R. Wilke, C. W. Tobias, and M. Eisenberg, "Free-Convection Mass Transfer at Vertical Plates," *Chem. Eng. Prog.*, 49 (1953), pp. 663-674.
6. K. Denpo, S. Teruta, Y. Fukunaka, and Y. Kondo, "Turbulent Natural Convection along a Vertical Electrode," *Metall. Trans. B*, 14B (1983), pp. 633-643.
7. A. A. Wragg, "Free Convection Mass Transfer at Horizontal Electrodes," *Electrochimica Acta*, 13 (1968), pp. 2159-2165.
8. A. A. Wragg and R. P. Loomba, "Free Convection Flow Patterns at Horizontal Surfaces with Ionic Mass Transfer," *Int. J. Heat Mass Transfer*, 13 (1970), pp. 439-442.
9. M. A. Patrick and A. A. Wragg, "Optical and Electrochemical Studies of Free Convection Mass Transfer at Horizontal Surfaces," *Int. J. Heat Mass Transfer*, 18 (1975), pp. 1397-1407.

10. M. A. Patrick, A. A. Wragg, and D. M. Pargeter, "Mass Transfer by Free Convection During Electrolysis at Inclined Electrodes," *Can. J. Chem. Eng.*, 55 (1977), pp. 432-438.
11. J. R. Selman and J. Tavakoli-Attar, "Free Convective Mass Transfer to a Rod-Shaped Vertical Electrode," *J. Electrochem. Soc.*, 127 (1980), pp. 1049-1055.
12. N. Ibl and R. H. Müller, "Studies of Natural Convection at Vertical Electrodes," *J. Electrochem. Soc.*, 105 (1958), pp. 346-353.
13. G. Wranglen, "Dendrites and Growth in the Electrocrystallization of Metals," *Electrochimica Acta*, 2 (1960), pp. 130-146.
14. J. T. Kim and J. Jorné, "The Kinetics and Mass Transfer of Zinc Electrode in Acidic Zinc-Chloride Solution," *J. Electrochem. Soc.*, 127 (1980), pp. 8-15.
15. C. Wagner, "Current Distribution in Galvanic Cells Involving Natural Convection," *J. Electrochem. Soc.*, 104 (1957), pp. 129-131.
16. N. Ibl, "Studies of Mass Transfer During Electrolysis with Natural Convection," *Proc. 8th Meeting Intern. Comm. Electrochem. Thermodynam. and Kinetics* (1958), pp. 174-189.
17. A. Damianovic, T. H. V. Setty, and J. O'M. Bockris, "Effect of Crystal Plane on the Mechanism and Kinetics of Copper Electrocrystallization," *J. Electrochem. Soc.*, 113 (1966), pp. 429-440.
18. J. L. Barton and J. O'M Bockris, "The Electrolytic Growth of Dendrites from Ionic Solutions," *Proc. Roy. Soc.*, A268 (1962), pp. 485-505.
19. D. R. Hamilton, "A Theory of Dendritic Growth in Electrolytes," *Electrochimica Acta*, 8 (1963), pp. 731-740.
20. A. R. Despic, J. W. Diggle, and J. O'M. Bockris, "Mechanism of the Formation of Zinc Dendrites," *J. Electrochem. Soc.*, 115 (1968), pp. 507-508.
21. J. W. Diggle, A. R. Despic, and J. O'M. Bockris, "The Mechanism of the Dendritic Electrocrystallization of Zinc," *J. Electrochem. Soc.*, 116 (1969), pp. 1503-1514.
22. F. Mansfield and S. Gilman, "The Effect of Potential and Time on Deposition Characteristics of Zinc on a Zinc Single Crystal in KOH," *J. Electrochem. Soc.*, 117 (1970), pp. 1521-1523.
23. U. Landau and B. D. Cahan, in "Zinc Electrodeposition and Dendritic Growth from Zinc Halide Electrolytes," Final Report EPRI-EM-2393, May 1982. P. C. Symons, editor.
24. A. R. Despic and M. M. Purenovic, "Critical Overpotential and Induction Time of Dendritic Growth," *J. Electrochem. Soc.*, 121 (1974), pp. 329-331.
25. R. Aogaki, K. Kitazawa, Y. Kose, and K. Fueki, "Theory of Powdered Crystal Formation in Electrocrystallization—Occurrence of Morphological Instability at the Electrode Surface," *Electrochim. Acta*, 25 (1980), pp. 965-972.
26. R. A. Huggins and D. Elwell, "Morphological Instability of a Plane Interface During Electrocrystallization from Molten Salts," *J. Crystal Growth*, 37 (1977), pp. 159-162.

27. D. Pletcher, Industrial Electrochemistry, Chapman and Hall, London, 1982.
28. G. Zwilling, D. M. Bailey, and K. A. Gschneidner, Jr., "Fused Salt Electrorefining of Gadolinium: an Evaluation of Three Electrolytes; II. Deposition Characteristics in LiCl-LiF-GdF₃, LiF-BaF₂-GdF₃, and LiF-GdF₃," J. Less-Common Metals, **78** (1981), pp. 109-118.
29. R. D. Naybour, "Morphologies of Zinc Electrodeposited from Zinc-Saturated Aqueous Alkaline Solution," Electrochim. Acta, **13** (1968), pp. 763-769.
30. R. D. Naybour, "The Effect of Electrolyte Flow on the Morphology of Zinc Electrodeposited from Aqueous Alkaline Solution Containing Zincate Ions," J. Electrochem. Soc., **116** (1969), pp. 520-524.
31. S. Goldsztaub and R. Itti, "Influence de la pesateur sur la repartition des concentrations autour d'un crystal en voie de croissance ou de décroissance," C. R. Acad. Sci. Paris, **262B** (1966), pp. 1291-1293.
32. L. A. Vasilev, Schlieren Methods, Keter Publishers Ltd., London (1971).
33. W. Merzkirch, "Density Sensitive Flow Visualization," in Methods of Experimental Physics: Fluid Dynamics, edited by R. J. Emrich, Vol. 18A, Academic Press, 1981, New York, pp. 345-403.
34. G. Wranglen, "A Shadow Schlieren Method for the Study of Diffusion Boundary Layers at Electrodes," Acta Chem. Scand., **12** (1958), pp. 1543-1544.
35. L. Stephenson and J. H. Bartlett, "Anodic Behavior of Copper in HCl," J. Electrochem. Soc., **101** (1954), pp. 571-581.
36. N. Ibl, "Methods for the Study of the Diffusion Layer," Proc. 7th Meeting Intern. Comm. Electrochem. Thermodynam. and Kinetics (1957), pp. 112-133.